JOC The Journal of Organic Chemistry

Article

pubs.acs.org/joc

Synthesis and Optical Properties of Imidazole- and Benzimidazole-Based Fused π-Conjugated Compounds: Influence of Substituent, Counteranion, and π-Conjugated System

Koji Takagi,*[,†] Kazuma Kusafuka,[†] Yohei Ito,[†] Koji Yamauchi,[†] Kaede Ito,[†] Ryoichi Fukuda,*[,‡,§] and Masahiro Ehara[‡,§]

[†]Department of Materials Science and Engineering, Graduate School of Engineering, Nagoya Institute of Technology, Gokiso, Showa, Nagoya 466-8555 Japan

[‡]Research Center for Computational Science, Institute for Molecular Science, 38 Nishigo-Naka, Myodaiji, Okazaki 444-8585 Japan

[§]Elements Strategy Initiative for Catalysts and Batteries, Kyoto University, Kyoto 615-8520 Japan

Supporting Information

ABSTRACT: Fused π-conjugated imidazolium chlorides having hydrogen (**1-Cl**), octyloxy (**2-Cl**), *N*,*N*-dibutylamino (**3-Cl**), trifluoromethyl (**4-Cl**), and cyano (**5-Cl**) groups substituted on the benzene ring at the 2-position of imidazole were prepared. Counteranion exchanges from chloride to bis(trifluoromethanesulfonyl)imidate (**2-TFSI**) and tetrafluoroborate (**2-BF4**) were performed. The optical properties of these compounds (absorption and emission wavelengths, fluorescence quantum yield, and solvatochromism) were influenced by both the substituent and anion character, which was investigated by theoretical calculations using the density functional theory (DFT) and symmetry-adapted cluster−configuration interaction (SAC−CI) methods. Fused π-conjugated benzimidazolium chlorides having *N*,*N*-dibutylamino (**6-Cl**) and cyano (**7-Cl**) groups were also prepared to observe the different solvatochromic shifts.

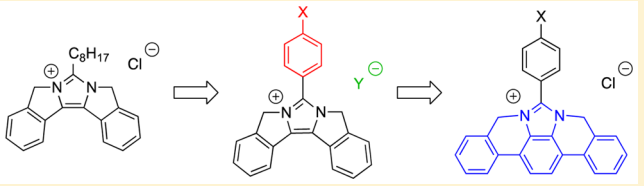

INTRODUCTION

π-Conjugated molecules have many fascinating properties such as light absorption, fluorescence emission, and charge transport, which leads to optoelectronic device applications including photovoltaic cells, light-emitting diodes, and field-effect transistors. The intrinsic character of π-conjugated molecules can be tuned by molecular design, and advancements in organic synthetic chemistry enable the preparation of numerous π-conjugated molecules. Especially, ladder and fused π-conjugated molecules[1] have attracted much attention because of the rigid and coplanar structure with restricted conformational change that gives rise to intriguing properties such as intense luminescence[2] and remarkable hole/electron mobility.[3] In addition to ladder and fused π-conjugated molecules comprised solely of the hydrocarbon skeleton, the incorporation of heteroatoms like sulfur (thiophene unit) influences the environmental stability and molecular packing structure, which contributes to improved device performance. Thus, the development of new fused oligothiophene derivatives and the understanding of structure−property relationships are the focus of interest in recent material chemistry.[4] Other fused π-conjugated molecules including heterole (borole, furan, silole, and phosphole units) are also attractive materials for optoelectronic applications.

On the other hand, imidazole is a versatile building block for the selective introduction of aromatic rings at the 1-, 2-, 4-, and 5-positions.[5] The transformation to imidazolium cation through alkylation at the 3-position further imparts photophysical,[6] chemical,[7] self-organizational,[8] catalytic,[9] and ion transport[10] properties. Accordingly, fused π-conjugated imidazolium compounds would be expected to act as novel functional materials. With this background in mind, we have previously synthesized two fused π-conjugated imidazolium compounds with rigid structures.[11] The compound with a methylene bridge (**0-Cl** in Figure 1) showed absorption and emission spectra with vibronic fine structure and relatively high fluorescence quantum yields; however, emission color-tuning was impossible due to limitations of the synthetic method.

We herein describe the synthesis of new fused π-conjugated imidazolium chlorides with electron-donating and -accepting substituents at the para position of the benzene ring at the 2-position of imidazole (**1-Cl**, **2-Cl**, **3-Cl**, **4-Cl**, and **5-Cl**). Exchange of the counteranion was also carried out (**2-TFSI** and **2-BF4**). In addition, fused π-conjugated benzimidazolium chlorides were synthesized (**6-Cl** and **7-Cl**). Absorption and emission wavelengths, fluorescence quantum yield, and solvatochromism were investigated in conjunction with theoretical calculations to examine the emission color-tuning possibility and understand the structure−property relationships of these compounds.

Received: May 13, 2015
Published: June 23, 2015

DOI: 10.1021/acs.joc.5b01028
J. Org. Chem. 2015, 80, 7172−7183

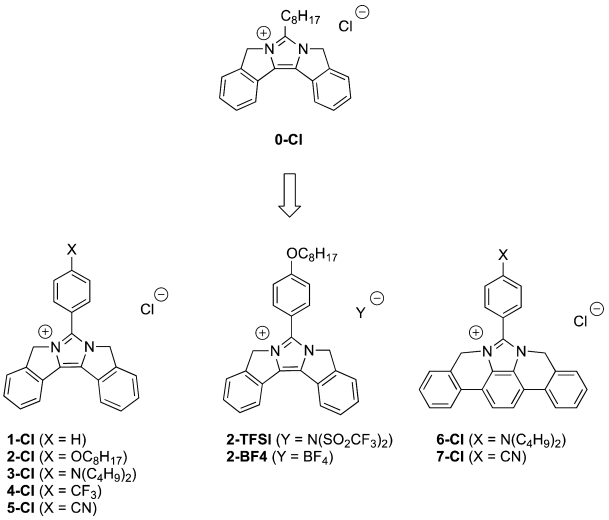

Figure 1. Chemical structure of fused π-conjugated imidazolium and benzimidazolium compounds, including **0-Cl** reported previously.

RESULTS AND DISCUSSION

Influence of Substituent. Initially, a fused π-conjugated imidazolium chloride (**1-Cl**) was synthesized from 2-phenylimidazole by bromination at the 4,5-positions, Suzuki coupling with 2-hydroxymethylphenylboronic acid, chlorination by $SOCl_2$, and lithium bis(trimethylsilyl)amide (LiHMDS)-promoted cyclization according to our previous report.[11] The double cyclization did not proceed effectively even when the reaction was performed in *N*,*N*-dimethylformamide (DMF). The single cyclization product was contaminated in the crude reaction mixture. Therefore, the solution of crude product in dimethyl sulfoxide (DMSO) was heated to complete the reaction, and **1-Cl** was finally obtained in 67% yield. UV−vis absorption and fluorescence emission spectra of acyclic 4,5-bis(2′-hydroxymethylphenyl)-2-phenylimidazole (**2**) and **1-Cl** were measured in MeOH (Figure 2). While the absorption

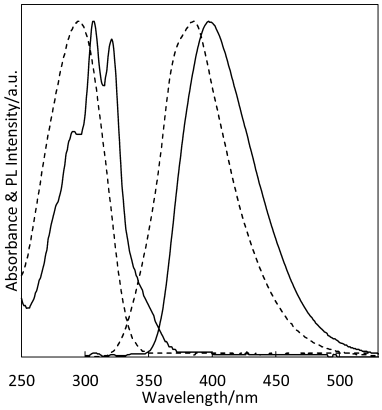

Figure 2. UV−vis absorption and fluorescence emission spectra of **2** (broken line) and **1-Cl** (solid line) in MeOH.

spectrum of **2** showed a smooth curve, that of **1-Cl** showed vibronic fine structure. Both the absorption and emission spectra of **1-Cl** (λ_{abs} at 321 nm and λ_{em} at 397 nm) exhibited bathochromic shifts from those of **2** (λ_{abs} at 294 nm and λ_{em} at 385 nm), and the fluorescence quantum yield was increased from 0.01 (**2**) to 0.29 (**1-Cl**). These results indicate the wide conjugation system of **1-Cl**. The absence of vibronic fine structure in the emission spectrum of **1-Cl** and the lower fluorescence quantum yield compared with **0-Cl** (0.62) could be ascribed to C−C bond rotation around the benzene (2-position) and imidazolium rings leading to emission from the energetically equivalent states and nonradiative decay processes, respectively.

Subsequently **2-Cl** and **3-Cl**, bearing the electron-donating octyloxy and *N*,*N*-dibutylamino groups, were synthesized from 1,2-bis(2′-(hydroxymethylphenyl)ethyne in five steps (Scheme 1). 4,5-Bis(2′-hydroxymethylphenyl)-2-arylimidazoles were prepared through imidazole ring formation from 1,2-diketone and aryl aldehyde derivatives because the bromination of electron-rich 2-arylimidazole compounds may suffer from undesirable reaction on the aryl ring instead of the imidazole ring. Methylene proton signals at the bridge point of **2-Cl** (5.88 ppm) and **3-Cl** (5.86 ppm) exhibited upfield shifts from **1-Cl** (5.93 ppm), suggesting the electron-rich character of the fused π-conjugated system.

UV−vis absorption and fluorescence emission spectra were measured in MeOH (Figure 3A). Absorption and emission maxima of **2-Cl** (λ_{abs} at 324 nm and λ_{em} at 395 nm) were comparable to those of **1-Cl**; however, the peak maxima of **3-Cl** (λ_{abs} at 349 nm and λ_{em} at 420 nm) were obviously red-shifted. The fluorescence quantum yields of **2-Cl** and **3-Cl** were 0.62 and 0.40, respectively. Density functional theory (DFT) calculations were performed by use of the Gaussian 09W program at the B3LYP/6-31G(d) level of theory to optimize the ground-state structure of the model compounds (**2′-Cl** and **3′-Cl**).[12] Dihedral angles between the imidazolium and benzene (2-position) rings of **2′-Cl** and **3′-Cl** were 38.5° and 34.4°, respectively, reflecting the pronounced charge transfer from the strong electron-donating *N*,*N*-dimethylaminophenyl group to the fused imidazolium cation unit in **3′-Cl**. Time-dependent (TD)-DFT calculations were then performed at the B3LYP/6-311+G(d,p) level of theory to estimate the vertical excitation (UV−vis absorption) energy. For **2′-Cl**, the one-electron transition with the largest oscillator strength (f = 0.492) was from the highest occupied molecular orbital (HOMO) to the second lowest unoccupied molecular orbital (LUMO + 1) (Figure 4; Table S1, Supporting Information). The frontier molecular orbital (FMO) of HOMO was spread over the entire molecule and that of LUMO + 1 was located on the fused imidazolium moiety. On the other hand, for **3′-Cl**, the important one-electron transition (f = 0.664) was from HOMO to LUMO. The FMOs of HOMO and LUMO were located on the *N*,*N*-dimethylaminophenyl and central imidazolium moieties, respectively, implying ane intramolecular charge-transfer characteristic. The smaller calculated one-electron transition energy of **3′-Cl** (3.76 eV) compared with **2′-Cl** (4.17 eV) agreed well with the observed red-shifted absorption spectrum of **3-Cl**.

4-Cl and **5-Cl**, bearing the electron-accepting trifluoromethyl and cyano groups, were likewise synthesized. Methylene proton signals at the bridge point of **4-Cl** and **5-Cl** (5.97 ppm) showed downfield shifts from **1-Cl**, suggesting the electron-poor character of the fused π-conjugated system. UV−vis absorption and fluorescence emission spectra were measured in MeOH (Figure 3B). Absorption maxima at around 305 and 320 nm were similarly observed for both compounds, but the absorbance at around 350 nm was considerably increased for **5-Cl**. The emission spectrum of **5-Cl** (λ_{em} at 448 nm) was red-shifted compared with that of **4-Cl** (λ_{em} at 417 nm). The fluorescence quantum yields of **4-Cl** and **5-Cl** were 0.41 and

DOI: 10.1021/acs.joc.5b01028
J. Org. Chem. 2015, 80, 7172−7183

Scheme 1. General Synthetic Route to Fused π-Conjugated Imidazolium Compounds[a]

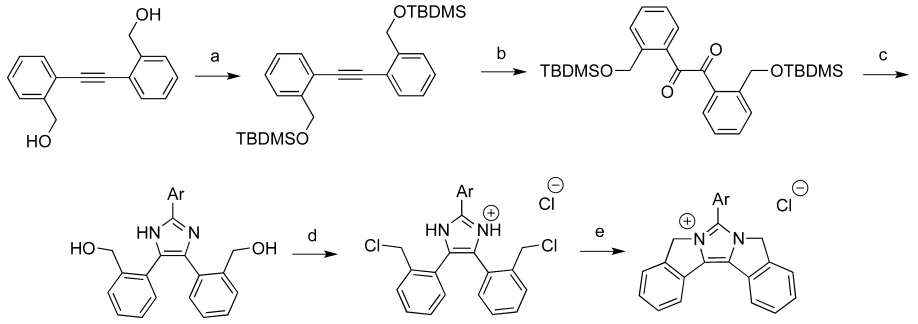

[a]Reagents and conditions: (a) TBDMSCl, imidazole, DMF, rt; (b) $KMnO_4$, $NaHCO_3$, $MgSO_4$, acetone/H_2O, rt; (c) ArCHO, NH_4OAc, L-proline, EtOH/DOX, reflux; (d) $SOCl_2$, MeCN, rt; (e) LiHMDS, DMF, rt, and then DMSO, 50 °C

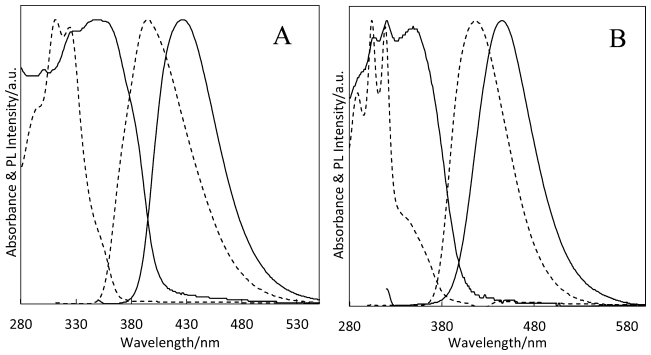

Figure 3. UV−vis absorption and fluorescence emission spectra of (A) **2-Cl** (broken line) and **3-Cl** (solid line) and (B) **4-Cl** (broken line) and **5-Cl** (solid line) in MeOH.

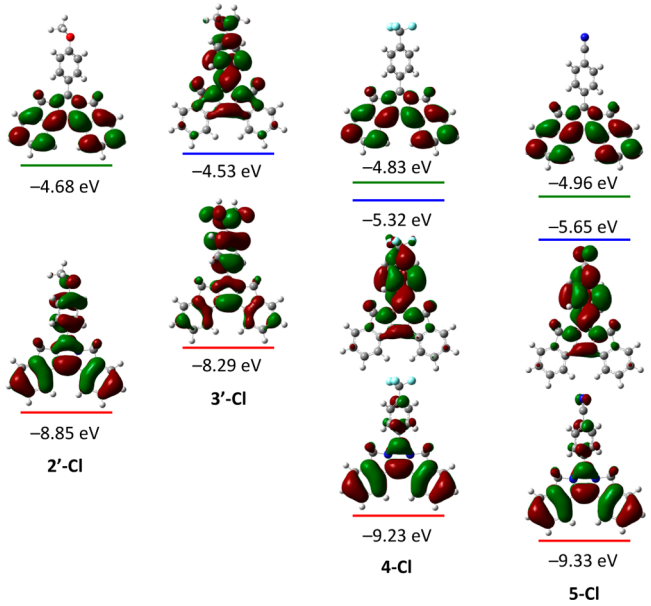

Figure 4. Frontier molecular orbital diagrams involved in the vertical excitation, calculated via TD-DFT//B3LYP/6-311+G(d,p), based on the optimized ground-state geometry. Red, blue, and green lines indicate energy levels of HOMO, LUMO, and LUMO + 1, respectively.

0.20, respectively. DFT (geometry optimization at the B3LYP/6-31G(d) level of theory) and TD-DFT (estimation of vertical excitation energy at the B3LYP/6-311+G(d,p) level of theory) calculations were performed for **4-Cl** and **5-Cl**, and the results are indicated in Figure 4 and Table S1 in Supporting Information. The one-electron transitions with the largest oscillator strength were always from HOMO to LUMO + 1. Both FMOs were distributed on the fused imidazolium moiety. On the other hand, the one-electron transition with the second-largest oscillator strength was from HOMO to LUMO, and the oscillator strength of **5-Cl** (f = 0.231) was larger than that of **4-Cl** (f = 0.187). From the FMO topologies, these HOMO−LUMO one-electron transitions indicate intramolecular charge transfer induced by the strong electron-accepting ability of the substituent. Bielawski and co-workers[6d] also described how installation of the 4-cyanophenyl group at the C1 position of imidazolium compound resulted in noticeable charge-transfer interacton. Accordingly, the theoretical TD-DFT calculation nicely accounts for the trend of UV−vis absorption spectra of these fused π-conjugated imidazolium compounds and is helpful to predict their optical properties, although there are some discrepancies between the calculated and experimental values.[13]

In order to deeply understand the optical properties of these compounds, UV−vis absorption and fluorescence emission spectra of **3-Cl** and **5-Cl** were measured in 1,4-dioxane (DOX), tetrahydrofuran (THF), acetone, DMF, DMSO, and acetonitrile (AN). Absorption spectra were affected by solvent character (Figure S20, Supporting Information); however, the influence was relatively small, and no clear relationships were observed against the orientational polarizability[14] or solvent dielectric. On the other hand, the emission wavelength of **5-Cl** was found to be more susceptible to solvent character and was gradually red-shifted with increasing solvent polarity (Figure 5B). Figure 5C shows the plots of Stokes shifts against Reichardt's solvent polarity parameters $E_T(30)$.[15] A larger positive solvatofluorochromic shift of **5-Cl** compared with **3-Cl** was obtained. The Stokes shifts ranged from 4620 cm^{-1} (DOX) to 5980 cm^{-1} (AN). This result is in sharp contrast to **0-Cl**, which exhibits negligible solvatochromic character,[11] and the intramolecular charge transfer might be responsible for the bathochromic shift of emission wavelength in polar solvents (vide infra). The fluorescence quantum yields were also dependent on solvent character (Table S2, Supporting Information). However, the results are difficult to explain because the solvent polarity influences not only intramolecular charge transfer but also cation−anion interaction, which is discussed in the next section.

Influence of Counteranion. We also performed anion exchange from chloride to bis(trifluoromethanesulfonyl)-imidate and tetrafluoroborate. Anion metathesis from chloride

DOI: 10.1021/acs.joc.5b01028
J. Org. Chem. 2015, 80, 7172−7183

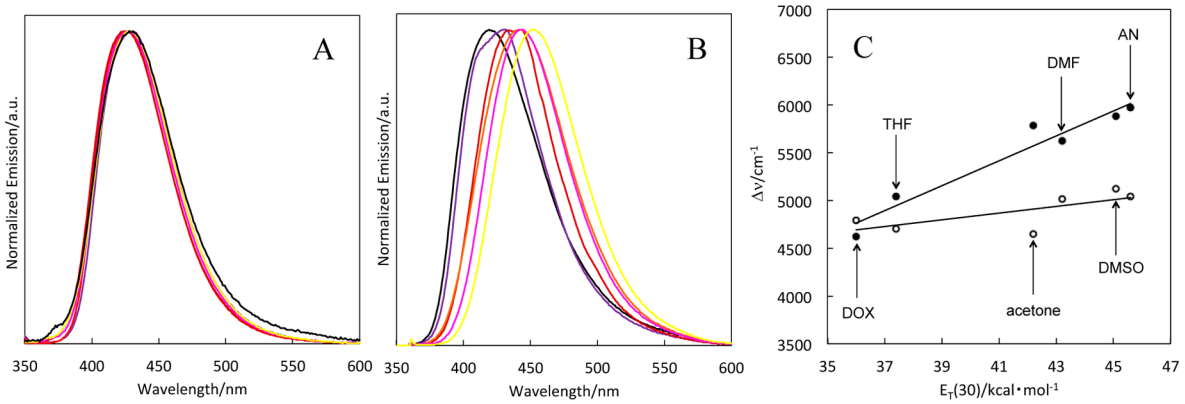

Figure 5. Fluorescence emission spectra of (A) **3-Cl** and (B) **5-Cl** in various solvents (black, DOX; purple, THF; red, acetone; pink, DMF; orange, AN; yellow, DMSO). (C) Plots of Stokes shifts against $E_T(30)$ values of solvents for (○) **3-Cl** and (●) **5-Cl**.

Scheme 2. General Synthetic Route to Fused π-Conjugated Benzimidazolium Compounds[a]

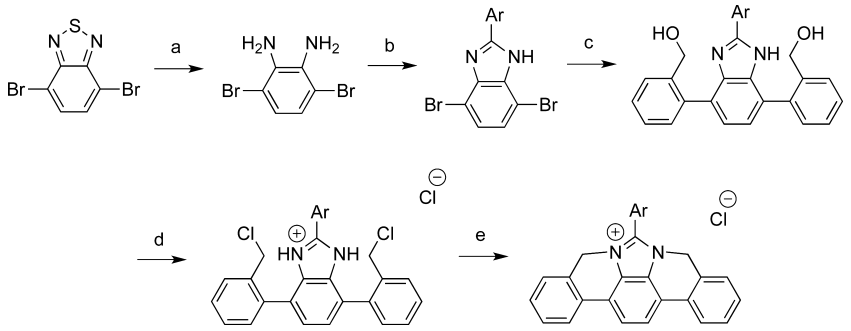

[a]Reagents and conditions: (a) $NaBH_4$, $CoCl_2$, THF/EtOH, reflux; (b) ArCHO, $ZrCl_4$, $CHCl_3$, rt; (c) 2-(hydroxymethyl)phenylboronic acid, $Pd(PPh_3)_4$, 2 M aqueous Na_2CO_3, THF, reflux; (d) $SOCl_2$, MeCN, rt; (e) LiHMDS, DMF, rt, and then DMSO, 50 °C

to bis(trifluoromethanesulfonyl)imidate was performed in a $CHCl_3$/water biphasic system, giving rise to **2-TFSI** simply by evaporation of the organic phase. Et_3OBF_4 was used for anion metathesis from chloride to tetrafluoroborate, following the protocol of Bielawski and co-workers.[16] Upon introduction of the bulky counteranion, the melting point was decreased from 255 °C (**2-Cl**) to 235 °C (**2-BF4**) and 126 °C (**2-TFSI**). Figure S16 (Supporting Information) shows the ^{1}H NMR spectra in $CDCl_3$ (2 mM, room temperature) of the three fused π-conjugated imidazolium compounds. The methylene proton signal at the bridge point exhibited a downfield shift from 5.08 ppm (**2-Cl**) to 5.42 ppm (**2-BF4**) and 5.51 ppm (**2-TFSI**). In the spectrum of **2-Cl**, the proton signals were generally broad. These results likely suggest that the chloride anion, in which the charge is localized on the chlorine atom, has the strongest interaction with imidazolium cation.[17] UV−vis absorption and fluorescence emission spectra were measured in THF (Figure S21, Supporting Information). The absorption spectra showed very small shifts upon changing the counteranion, and tailing to the longer wavelength was observed only for **2-Cl**. Because the emission spectra were completely overlapped, the fused π-conjugated imidazolium cation should be the emissive core. On the other hand, the fluorescence quantum yield was dependent on the counteranion. The low fluorescence quantum yield of **2-Cl** (0.31) was improved upon introduction of counteranions with weak coordination ability, namely, 0.45 for **2-BF4** and 0.62 for **2-TFSI**. Matsumoto et al.[6j] also reported similar results for diimidazoquinoxalinium salts. The orders of methylene proton chemical shifts and fluorescence quantum yields are in good accordance with each other. Therefore, it can be considered that strong interaction between fused π-conjugated imidazolium cation and chloride anion in **2-Cl** results in nonradiative decay from the excited state, particularly in less polar THF. In polar MeOH solution, on the other hand, the ionic species separate by solvation to suppress the nonradiative decay, recovering the relatively high fluorescence quantum yield (0.62).

Influence of π-Conjugated System. As mentioned above, fused π-conjugated imidazolium compounds are potential candidates for fluorescent materials. Emission wavelength can be tuned by the substituent, and emission intensity can be controlled by the counteranion. Fused benzimidazolium compounds were synthesized to extend the effective conjugation length and compare their absorption/emission behavior with that of fused imidazolium compounds. Herein, **6-Cl** and **7-Cl** bearing *N*,*N*-dibutylamino and cyano groups, respectively, were prepared following Scheme 2. Acyclic precursors bearing the 2-hydroxymethylphenyl group were obtained by Suzuki coupling reaction of 2-aryl-4,7-dibromo-1*H*-benzimidazole with 2-hydroxymethylphenylboronic acid. After chlorination with $SOCl_2$, 2-aryl-4,7-bis(2′-chloromethylphenyl)-1*H*-benzimidazolium chloride was treated with LiHMDS to give the fused π-conjugated benzimidazolium chlorides. Chemical shifts of the methylene proton at the bridge point of **6-Cl** and **7-Cl** were comparable with those of **3-Cl** and **5-Cl** bearing the same substituent.

Figure 6 shows UV−vis absorption and fluorescence emission spectra of compounds consisting of the same substituent and different π-conjugated systems in MeOH. Both the absorption and emission spectra of **6-Cl** (λ_{abs} at 368

DOI: 10.1021/acs.joc.5b01028
J. Org. Chem. 2015, 80, 7172−7183

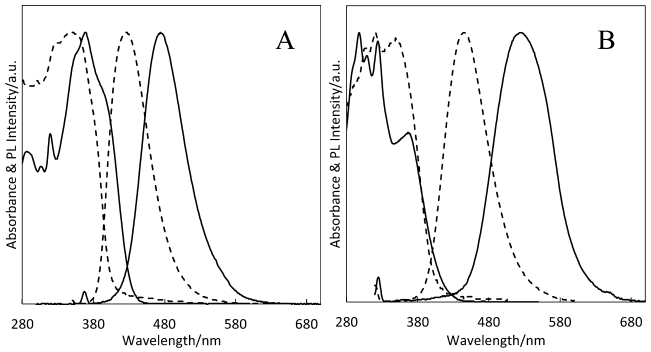

Figure 6. UV−vis absorption and fluorescence emission spectra of (A) **3-Cl** (broken line) and **6-Cl** (solid line) and (B) **5-Cl** (broken line) and **7-Cl** (solid line) in MeOH.

nm and λ_{em} at 474 nm) showed bathochromic shifts compared with those of **3-Cl** (Figure 6A). Unexpectedly, the fluorescence quantum yield of **6-Cl** was quite low (0.03). From the DFT calculation of a model compound (**6′-Cl**) at the B3LYP/6-31G(d) level of theory, the dihedral angle between benzimidazolium and benzene (2-position) rings was 47.8°, which is larger than that of **3′-Cl** (34.4°). Accordingly, the photoinduced electron transfer (PET) from the *N*,*N*-dibutylaminophenyl moiety to the emissive benzimidazolium core might be a plausible reason to quench the fluorescence emission,[18] which is carefully discussed by use of symmetry-adapted cluster−configuration interaction (SAC−CI) calculation in the following section. The oscillator strength of fluorescence for **6′-Cl** calculated by the SAC−CI method is distinguishably smaller than that for **3′-Cl**, reflecting the long-distance electron transfer induced by the photoemission. The absorption spectrum of **7-Cl** did not exhibit an apparent bathochromic shift from **5-Cl**, but the peak at 367 nm with medium intensity was red-shifted compared with the peak maximum (λ_{abs} at 349 nm) of **5-Cl** (Figure 6B). The DFT calculation was performed for **7-Cl** to find out that the dihedral angle between benzimidazolium and benzene (2-position) rings was 57.0°, which is larger than that of **5-Cl** (44.7°). This result is similar to the relationship of **3′-Cl** and **6′-Cl**. The emission spectrum of **7-Cl** (λ_{em} at 524 nm) was obviously red-shifted compared with **5-Cl**, and the fluorescence quantum was low (0.03).

The solvatochromic behaviors of **6-Cl** and **7-Cl** were examined by collecting UV−vis absorption (Figure S22, Supporting Information) and fluorescence emission spectra in various solvents. Both **6-Cl** and **7-Cl** had larger Stokes shifts compared with the fused π-conjugated imidazolium compounds (**3-Cl** and **5-Cl**), although the spectra of **7-Cl** in DOX and THF could not be obtained due to its low solubility. As indicated in Figure 7, **6-Cl**, having the electron-donating *N*,*N*-dimethylamino group, exhibited a clear positive solvatofluorochromic shift, which is in contrast to the trend observed for **3-Cl** (Figure 5). The Stokes shifts ranged from 5140 cm^{-1} (DOX) to 6770 cm^{-1} (DMSO).

SAC−CI Calculations. For detailed analyses and deep understanding of substituent and π-conjugation effects, we performed highly accurate quantum chemical calculations by using the SAC−CI method[19] for the cationic frameworks of **3′-Cl**, **5-Cl**, **6′-Cl**, and **7-Cl**, where the amino group of **3-Cl** and **6-Cl** was replaced by -N$(CH_3)_2$. Tables S4 and S5 (Supporting Information) show the low-lying UV−vis absorptions calculated by the SAC−CI method. The results in gas phase as well as in solutions (DOX and AN) are shown. Solvent effects were considered by the polarizable continuum model (PCM) SAC−CI method.[20] The stick absorption spectra are shown in Figure 8. For **3′-Cl**, the 1^1A state calculated around 350 nm corresponds to the observed absorption. The SAC−CI calculation indicates that this state exhibits a positive solvatochromic shift due to the charge-transfer excitation character; however, a significant solvatochromic shift was not observed in the measured spectra. For **5-Cl**, the 1^1A state calculated around 320 nm corresponds to the observed absorption with negligible solvatochromic shifts. The observed solvatochromic shift was also small.

For **6′-Cl**, small absorptions of the 1^1A state were calculated around 450 nm in DOX and AN solutions. These states must correspond to the observed peak shoulder around 410 nm, although the SAC−CI calculations underestimated the excitation energy by about 0.25 eV. The intensity of this state is small because the weight of two-electron excitations becomes large. Namely, this state has a singlet biradical character to some extent. Interestingly, this biradical-like state was not obtained by the SAC−CI calculation in gas phase. More detailed computations are necessary for understanding this biradical-like state; however, such study is beyond the purpose of this paper and will be reported in the future. The main peak of **6′-Cl** observed around 350 nm is assignable to the 1^1B state.

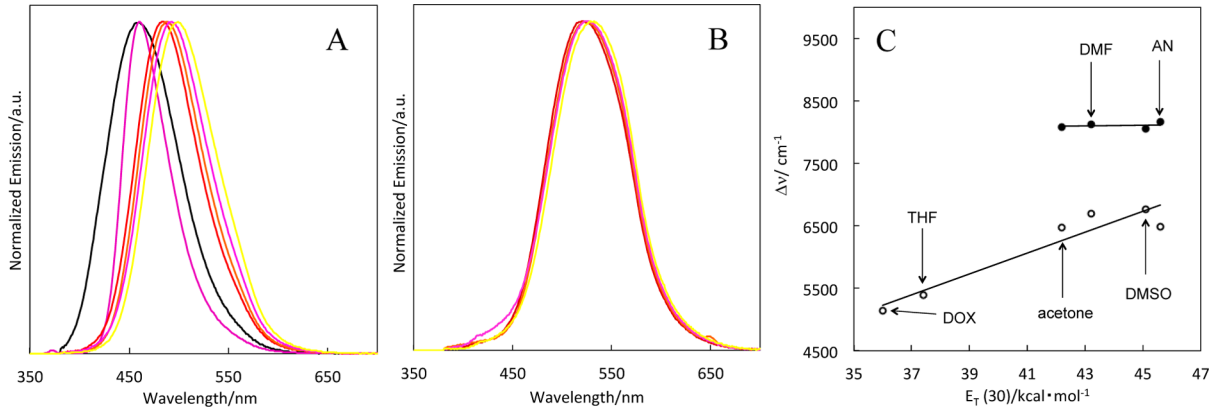

Figure 7. Fluorescence emission spectra of (A) **6-Cl** and (B) **7-Cl** in various solvents (black, DOX; purple, THF; red, acetone; pink, DMF; orange, AN; yellow, DMSO). (C) Plot of Stokes shifts against $E_T(30)$ values of solvents for (○) **6-Cl** and (●) **7-Cl**.

DOI: 10.1021/acs.joc.5b01028
J. Org. Chem. 2015, 80, 7172−7183

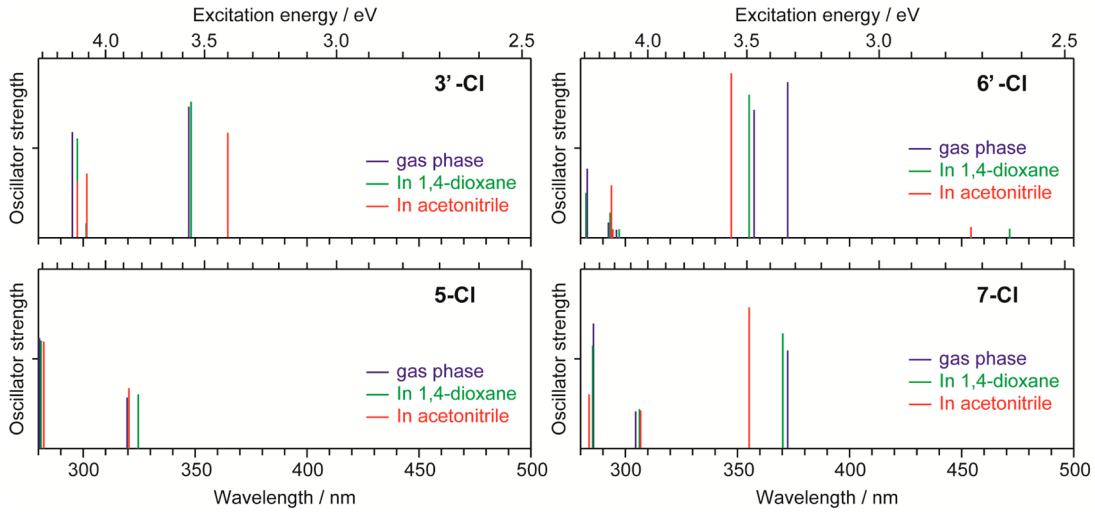

Figure 8. SAC−CI spectra for **3′-Cl**, **5-Cl**, **6′-Cl**, and **7-Cl** in gas phase, 1,4-dioxane, and acetonitrile.

Table 1. Emission Energy and Fluorescence Wavelengths of 3′-Cl, 5-Cl, 6′-Cl, and 7-Cl[a]

	3'-Cl		5-Cl		6'-Cl		7-Cl	
	1^1A	1^1B	1^1A	1^1B	1^1A	1^1B	1^1A	1^1B
	EE / Flu	EE / Flu	EE / Flu	EE / Flu	EE / Flu	EE / Flu	EE / Flu	EE / Flu
Gas phase	2.99 / 415 (1.286)[b]	3.88 / 319 (1.425)[b]	3.23 / 384 (0.774)[b]	3.98 / /312 (1.700)[b]	4.27 / 290 (0.223)[b]	2.84 / 437 (0.411)[b]	3.42 / 363 (1.139)[b]	2.41 / 515 (0.262)[b]
DOX	3.01 / 412	3.70 / 335	3.11 / 399	3.95 / 314	3.85 / 322	3.06 / 405	3.29 / 376	2.46 / 504
AN	2.77 / 447	2.95 / 421	2.87 / 433	3.76 / 329	2.42 / 512	3.06 / 405	2.19 / 566	2.03 / 611
Exp (DOX)	2.89 / 429		2.96 / 419		2.70 / 460		NA	
Exp (AN)	2.92 / 425		2.81 / 441		2.55 / 487		2.37 / 524	

[a]Calculated by the SAC−CI method for the lowest ^{1}A and ^{1}B states in gas phase, 1,4-dioxane (DOX), and acetonitrile (AN). Experimental results in DOX and AN are also given. [b]Oscillator strength.

For **7-Cl**, the 1^1B state calculated around 370 nm corresponds to the observed absorption. The SAC−CI calculation indicates that this state exhibits a negative solvatochromic shift. In comparison with **3′-Cl** and **5-Cl**, the absorptions of **6′-Cl** and **7-Cl** are generally calculated at lower energy with higher intensity. These findings are the results of extending the π-conjugated systems. Comparing the **5-Cl** and **7-Cl** results with **3′-Cl** and **6′-Cl** ones, we may find the substituent effect of −CN and -N$(CH_3)_2$. The 1^1A states exhibit a high-energy shift by substitution with the CN group. As a result, the lowest state of **7-Cl** is changed to the 1^1B state. These findings result in substituent effects on the HOMO and LUMO; the electron-withdrawing ability of CN group tends to localize the HOMO and LUMO to imidazolium (benzimidazolium) and Ar−CN moieties, respectively, as we found in the DFT calculations.

Table 1 shows the emission energies and fluorescence wavelengths of **3′-Cl**, **5-Cl**, **6′-Cl**, and **7-Cl** calculated by the SAC−CI method for the lowest ^{1}A and ^{1}B states. Both states are optically allowed, and therefore the observed fluorescence is emitted from the lower one. For **3′-Cl** and **5-Cl**, the lowest state is 1^1A, while the lowest state of **7-Cl** is 1^1B. The calculated oscillator strengths of fluorescence are 1.286, 0.774, 0.411, and 0.262 for **3′-Cl**, **5-Cl**, **6′-Cl**, and **7-Cl**, respectively, in gas phase. Although the fluorescence quantum yield is given by a competition of several relaxation pathways, the calculated oscillator strengths indicate the importance of electron-transfer quenching processes for these series of compounds. Indeed, the differences of electric dipole momenta between the emissive and ground states are 2.23, 10.77, 11.33, and 12.30 (Debye) for **3′-Cl**, **5-Cl**, **6′-Cl**, and **7-Cl**, respectively, calculated by the SAC−CI method in gas phase. These values indicate that the electron distribution of **6′-Cl** is significantly changed by the fluorescence due to its charge-transfer (CT) transition character. In accordance with the electric dipole moment, the CT character of **6′-Cl** is as large as those of cyano-substituted **5-Cl** and **7-Cl**. Those fluorescence transitions are calculated to be the HOMO−LUMO transition (the orbital diagram is given in Figure S23 in Supporting Information). The distributions of HOMO and LUMO are significantly different; therefore, the transition dipole and oscillator strength of **6′-Cl** become small in comparison with those of **3′-Cl**. For **6′-Cl**, 1^1B is the lowest state in gas phase or less polar environment; however, 1^1A shifts to the lowest state in polar solutions. Therefore, the emission state of **6-Cl** is altered by the polarity of solvent

DOI: 10.1021/acs.joc.5b01028
J. Org. Chem. 2015, 80, 7172−7183

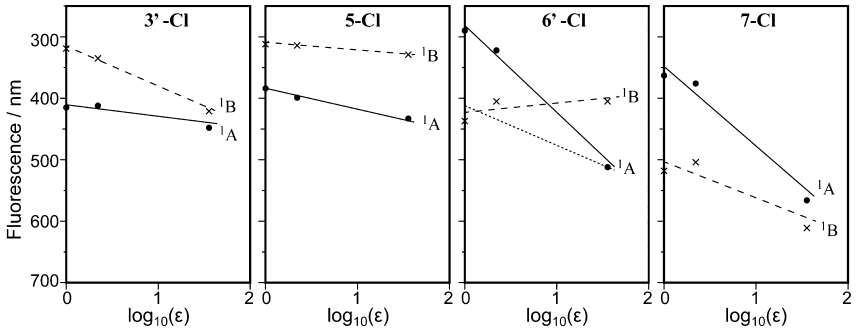

Figure 9. Solvent dependence of fluorescence wavelengths with respect to the logarithm of the dielectric constant of solvent (ε).

environment that must be responsible for the significant solvatofluorochromic shift. The calculated emission energies of **3′-Cl** and **5-Cl** agree well with experimental observations. The calculated results of **6′-Cl** and **7-Cl** reasonably agree with experiment.

The calculated solvatochromic shifts of fluorescence are shown in Figure 9 with respect to the logarithm of the dielectric constant (ε) of the solvent: ε = 1.0 for gas phase, ε = 2.21 for DOX, and ε = 35.69 for AN. The calculated solvatochromic shifts correlate better with ε than $E_T(30)$ values because the solvent is modeled by ε in the PCM calculations; $E_T(30)$ contains all kind of solvent effects, and some of them are not considered by PCM. Although the calculated number of solvents is limited, we found the following tendencies of solvatofluorochromic shifts: (1) The fluorescence solvatochromic shift of **5-Cl** is larger than that of **3′-Cl** (emission from 1^1A states, shown by solid lines). (2) For **6′-Cl**, we obtain tafluorescence solvatochromic shift whose extent is larger than **5-Cl** (dotted line is drawn with the approximation of two crosses and one circle). These findings agree well with experiment. According to the SAC−CI calculations, **7-Cl** is expected to show a fluorescence solvatochromic shift similar to **6′-Cl** (emission from 1^1B states, shown by dashed lines), although its low solubility restricts the experimental measurement. The fluorescence solvatochromic shift of the 1^1A state is significant for the larger π-conjugated systems of **6′-Cl** and **7-Cl**. This indicates that charge transfer in the 1^1A state is enhanced by extending the π-conjugation.

The calculated Stokes shifts are shown in Table 2. The SAC−CI results well reproduced the observed trends. The solvent dependence of the Stokes shift is remarkably small for **3′-Cl** because the absorption maximum and fluorescence energies exhibit similar positive solvatochromic shifts. The absorption maxima of **5-Cl**, **6′-Cl**, and **7-Cl** exhibit rather small negative solvatochromic shifts, and this enhances the solvent dependence of Stokes shifts.

Table 2. Calculated Stokes Shifts for 3′-Cl, 5-Cl, 6′-Cl, and 7-Cl in Gas Phase, 1,4-Dioxane, and Acetonitrile

	calcd Stokes shifts (cm^{-1})			
	3′-Cl	**5-Cl**	**6′-Cl**	**7-Cl**
gas phase	4678	5243	3952	7420
DOX	4436	5727	3468[a]	7718
AN	5081	8066	9275[a]	11776
Δ(AN − DOX)[b]	645	2339	5807	4597

[a]Absorption maximum is the 1^1B state. [b]Difference in calculated Stokes shifts between AN and DOX.

Table 3 shows the dihedral angles and bond lengths between imidazolium (benzoimidazolium) and benzene (2-position) rings of the optimized geometries used for the SAC−CI calculations. Except for the 1^1A state of **6′-Cl**, dihedral angles in the excited state are smaller than those in the ground state. The conjugation between imidazolium (benzoimidazolium) and benzene rings is enhanced in the excited states. Indeed, the bond lengths between imidazolium (benzoimidazolium) and benzene are shortened by about 0.05 Å upon going from the ground state to the excited state. In gas phase, the dihedral angle of **6′-Cl** in the 1^1A state is 87.9°, indicating that the molecule has a twisted structure. Thus, this molecule is expected to show a twisted intramolecular charge transfer (TICT) phenomenon. The TICT structure is quite solvent-sensitive. Namely, the twisted structure is significantly relaxed even in less polar DOX solution. In AN solution, the dihedral angle in the 1^1A state is smaller than that in the ground state; therefore, **6′-Cl** takes local excited states in AN solution similar to the other molecules. As shown in Table 1 and Figure 9, the emission state of **6′-Cl** is altered by the polarity of solvent. The solvent-depended TICT structure is the origin of this characteristic findings of the fluorescence of **6′-Cl**.

■ CONCLUSIONS

We have successfully prepared a set of fused π-conjugated imidazolium and benzimidazolium compounds bearing electron-donating and -accepting substituents. Anion exchange was also carried out. For a family of imidazolium derivatives, the absorption/emission properties and fluorescence quantum yield were influenced by the substituents. These results can be nicely reproduced on the basis of the optimized ground-state structure and estimated vertical excitation energy obtained by DFT and TD/DFT calculations, respectively. Compounds bearing the strongly electron-accepting cyano group exhibited pronounced positive solvatofluorochromism. The counteranion impacted the fluorescence quantum yield. In contrast to imidazolium derivatives, the benzimidazolium bearing the strongly electron-donating *N*,*N*-dibutylamino group demonstrated a marked positive solvatofluorochromic shift. For accurate understanding of these curious solvatofluorochromic behaviors, SAC−CI calculations were conducted both in gas phase and in solutions. The presented molecules have C_2 symmetry, and therefore lowest ^{1}A and ^{1}B states can be relevant to the absorption and fluorescence. For imidazolium compounds, the ^{1}A state has much lower energies than the ^{1}B state. For benzimidazolium compounds, on the other hand, the ^{1}B state is stabilized and is relevant to absorption and fluorescence. The electron-withdrawing ability of cyano group affects the localized electron distributions of the valence orbitals. The presented molecules

DOI: 10.1021/acs.joc.5b01028
J. Org. Chem. 2015, 80, 7172−7183

Table 3. Optimized Dihedral Angles and Bond Lengths between Imidazolium (Benzimidazolium) and Benzene (2-Position) Rings[a]

	3′-Cl			5-Cl			6′-Cl			7-Cl		
	GS[b]	1^1A	1^1B	GS[b]	1^1A	1^1B	GS[b]	1^1A	1^1B	GS[b]	1^1A	1^1B
						Dihedral Angle (deg)						
gas	34.9	21.6	32.2	43.9	25.6	33.3	48.0	87.9	26.5	57.3	31.8	29.9
DOX	35.7	19.4	27.4	44.0	23.3	34.6	47.0	55.6	32.8	56.4	31.7	31.2
AN	35.3	16.0	22.1	40.6	18.8	35.8	47.0	42.1	41.7	57.1	30.2	32.3
						Bond Length (Å)						
gas	1.449	1.407	1.453	1.464	1.411	1.446	1.453	1.478	1.401	1.469	1.408	1.407
DOX	1.450	1.405	1.440	1.465	1.410	1.449	1.452	1.462	1.415	1.470	1.405	1.410
AN	1.451	1.401	1.431	1.464	1.407	1.451	1.453	1.440	1.437	1.470	1.400	1.415

[a]For **3′-Cl**, **5-Cl**, **6′-Cl**, and **7-Cl** in gas phase, 1,4-dioxane (DOX), and acetonitrile (AN) for the ground and lowest excited states. [b]Ground state.

have a positive charge; therefore, solvent effects significantly stabilize the explicit charge in the initial state. The solvatochromic behavior may slightly differ from that in neutral molecules in which the solvation of electric dipole is dominant.

EXPERIMENTAL SECTION

4,5-Dibromo-2-phenylimidazole (1).[21] To a solution of 2-phenylimidazole (2.0 g, 14 mmol) in DMF (76 mL) was added *N*-bromosuccinimide (NBS; 4.8 g, 27 mmol) at 0 °C in the dark, and the mixture was stirred overnight at room temperature. After the solvent was removed, water and ethyl acetate were added in the separating funnel. An aqueous phase was extracted with ethyl acetate. The combined organic phase was rinsed with saturated aqueous $Na_2S_2O_3$ and dried over $MgSO_4$. The solvent was removed and the remaining solid was washed with hexane to obtain **1** (3.0 g, 72% yield). Colorless solid; mp 139−140 °C; ^{1}H NMR (200 MHz, DMSO-d_6) δ ppm 7.29−7.55 (m, 3H), 7.88 (d, J = 7.58 Hz, 2H), 13.61 (br s, 1H).

4,5-Bis(2′-hydroxymethylphenyl)-2-phenylimidazole (2). To a solution of **1** (0.40 g, 1.3 mmol) and 2-hydroxymethylphenylboronic acid (0.61 g, 4.0 mmol) in THF (24 mL) were added 2 M aqueous Na_2CO_3 (5.7 mL) and $Pd(PPh_3)_4$ (77 mg, 67 μmol), and the mixture was heated to reflux overnight. After the solvent was removed, water and ethyl acetate were added in the separating funnel. An aqueous phase was extracted with ethyl acetate. The combined organic phase was rinsed with saturated aqueous NH_4Cl and dried over Na_2SO_4. The solvent was removed and the remaining solid was purified by SiO_2 column chromatography (ethyl acetate/hexane = 1:1, R_f = 0.3) to obtain **2** (0.33 g, 70% yield). Colorless solid; mp 159−160 °C; ^{1}H NMR (400 MHz, DMSO-d_6) δ ppm 4.14−4.28 (m, 2H), 4.46−4.54 (m, 2H), 5.14−5.32 (m, 1H), 6.11−6.21 (m, 1H), 6.92 (d, J = 7.03 Hz, 1H), 7.03−7.10 (m, 1H), 7.22−7.26 (m, 1H), 7.32 (br s, 2H), 7.40−7.42 (m, 1H), 7.47−7.60 (m, 5H), 7.97−8.01 (m, 1H); ^{13}C NMR (50 MHz, DMSO-d_6) δ ppm 125.4, 127.1, 129.0, 129.4, 130.3, 145.2; IR (attenuated total reflectance, ATR) cm^{-1} 3738.3, 323.07, 3064.3, 2959.2, 2869.7, 2865.3, 1598.7, 1464.8, 1309.4, 1006.7, 963.3, 761.7. Anal. Calcd for $C_{23}H_{20}N_2O_2\cdot0.5H_2O$: C, 75.60; H, 5.79; N, 7.67. Found: C, 75.88; H, 5.60; N, 7.65.

1,3-Dihydro-4,5-bis(2′-chloromethylphenyl)-2-phenylimidazolium Chloride (3). To a solution of **2** (0.27 g, 0.76 mmol) in CH_3CN (68 mL) was added $SOCl_2$ (15 mL, 0.21 mol), and the mixture was stirred overnight at room temperature. After the solvent was removed, the remaining solid was washed with hexane to obtain **3** (0.20 g, 76% yield). Colorless solid; mp >350 °C; ^{1}H NMR (200 MHz, $CDCl_3$) δ ppm 0.84 (br s, 6H), 1.60 (br s, 4H), 3.53 (br s, 4H), 4.67−4.77 (m, 4H), 7.19−7.57 (m, 12H); ^{13}C NMR (50 MHz, DMSO-d_6) δ ppm 44.7, 124.2, 127.1, 127.9, 129.1, 129.4, 129.7, 130.8, 131.0, 132.1, 132.3, 137.8, 144.6; IR (ATR) cm^{-1} 3853.1, 3735.4, 3058.6, 2868.6, 2718.2, 2562.0, 2342.1, 1644.0, 1484.0, 1321.0, 1164.0, 1035.6, 764.6, 706.8, 676.9.

Phenyl-Substituted Fused Imidazolium Chloride (1-Cl). To a solution of **3** (0.11 g, 0.25 mmol) in DMF (25 mL) was added 1.0 M THF solution of LiHMDS (0.5 mL, 0.5 mmol) at 0 °C, and the mixture was stirred overnight at room temperature. After the solvent was removed, water and $CHCl_3$ were added in the separating funnel. An aqueous phase was extracted with $CHCl_3$. The combined organic phase was rinsed with sat. aqueous NH_4Cl and dried over $MgSO_4$. The solvent was removed and the remaining solid was dissolved in DMSO (16 mL) to be heated to 50 °C for 5 h. After the solvent was removed, the remaining solid was dissolved in $CHCl_3$ to be poured in ethyl acetate/hexane mixed solvent ($CHCl_3$: ethyl acetate: hexane =1:2:5) to obtain **1-Cl** (60 mg, 67% yield). Brown solid; mp >350 °C; ^{1}H NMR (400 MHz, DMSO-d_6) δ ppm 5.93 (brs, 4H), 7.63−7.82 (m, 9H), 8.27 (d, J = 6.78 Hz, 4H); ^{13}C NMR (100 MHz, DMSO-d_6) δ ppm 44.7, 122.3, 122.7, 124.8, 127.3, 128.2, 129.7, 129.9, 130.2, 133.1, 138.3, 140.9; IR (ATR) cm^{-1} 3445.21, 3053.7, 2912.9, 2847.4, 2217.7, 1664.3, 1579.4, 1140.7, 996.1, 888.1, 764.6, 721.2, 695.2. Electrospray ionization quadrupole time-of-flight high-resolution mass spectrometry [HRMS (ESI/TOF-Q)] m/z [**1-Cl** − Cl]$^+$ calcd for $C_{23}H_{17}N_2$, 321.1386; found, 321.1411; Anal. Calcd for $C_{23}H_{17}ClN_2\cdot2.9H_2O$: C, 67.53; H, 5.62; N, 6.85; Found: C, 67.84; H, 5.32; N, 7.08.

1,2-Bis[2′-(*t*-butyldimethylsiloxymethyl)phenyl]ethyne (4). To a solution of 1,2-bis[2′-(hydroxymethyl)phenyl]ethyne[2] (1.9 g, 7.7 mmol) in DMF (30 mL) were added imidazole (3.0 g, 31 mmol) and *t*-butyldimethylsilyl chloride (2.1 g, 20 mmol), and the mixture was stirred overnight at room temperature. After the solvent was removed, water and ethyl acetate were added in the separating funnel. An aqueous phase was extracted with ethyl acetate. The combined organic phase was dried over $MgSO_4$. The solvent was removed and the remaining solid was extracted with hexane to obtain **4** (3.6 g, quantitative yield). Colorless oil; ^{1}H NMR (200 MHz, $CDCl_3$) δ ppm 0.13 (s, 12H), 0.97 (s, 18H), 4.98 (s, 4H), 7.26−7.64 (m, 8H).

1,2-Bis[2′-(*t*-butyldimethylsiloxymethyl)phenyl]ethane-1,2-dione (5). To a mixture of **4** (3.7 g, 8.2 mmol), $NaHCO_3$ (1.1 g, 14 mmol), $MgSO_4$ (2.0 g, 17 mmol) in acetone (240 mL), and water (160 mL) was added $KMnO_4$ (5.1 g, 32 mmol), and the mixture was stirred overnight at room temperature. An aqueous phase was extracted with CH_2Cl_2, and the combined organic phase was dried over $MgSO_4$. The solvent was removed and the remaining solid was rinsed with CH_3OH to obtain **5** (1.8 g, 43% yield). Colorless solid; mp 135−136 °C; ^{1}H NMR (200 MHz, $CDCl_3$) δ ppm 0.16 (s, 12H), 0.99 (s, 18H), 5.25 (s, 4H), 7.21−7.42 (m, 2H), 7.57−7.74 (m, 4H), 7.99 (d, J = 7.83 Hz, 2H); ^{13}C NMR (50 MHz, $CDCl_3$) δ ppm 18.5, 26.1, 63.5, 126.5, 126.9, 129.3, 133.1, 134.4, 146.0, 196.6; IR (ATR) cm^{-1} 2948.6, 2925.5, 2854.1, 1656.6, 1600.6, 1570.7, 1458.9, 1251.6, 1199.5, 809.0, 777.3, 724.1, 668.2, 648.9. HRMS (ESI/TOF-Q) m/z [**5** + Na]$^+$ calcd for $C_{28}H_{42}NaO_4Si_2$, 521.2519; found, 521.2519.

4,5-Bis[2′-(hydroxymethyl)phenyl]-2-(4″-octyloxyphenyl)-imidazole (6). A mixture of **5** (0.30 g, 0.60 mmol), 4-octyloxybenzaldehyde (0.17 mL, 0.72 mmol), L-proline (10 mg, 0.09 mmol), and ammonium acetate (1.4 g, 18 mmol) in EtOH (2.4 mL) and 1,4-dioxane (1.2 mL) was heated to reflux overnight. Water was added and an aqueous phase was extracted with ethyl acetate. The combined organic phase was rinsed with saturated aqueous NH_4Cl and dried over $MgSO_4$. The solvent was removed and the remaining solid was dissolved in $CHCl_3$ to be poured in hexane to obtain **6** (0.21 g,

DOI: 10.1021/acs.joc.5b01028
J. Org. Chem. 2015, 80, 7172−7183

72% yield). Colorless solid; mp 163−164 °C; ^{1}H NMR (200 MHz, DMSO-d_6) δ ppm 0.85−0.94 (m, 3H), 1.31 (br s, 10H), 1.73−1.84 (m, 2H), 3.98 (t, J = 6.44 Hz, 2H), 4.69 (s, 4H), 6.95 (d, J = 8.59 Hz, 2H), 7.07−7.20 (m, 4H), 7.29 (br s, 2H), 7.44 (d, J = 7.58 Hz, 2H), 7.77 (d, J = 8.59 Hz, 2H); ^{13}C NMR (50 MHz, CD_3OD) δ ppm 13.1, 22.4, 25.8, 29.0, 29.1, 31.6, 62.5, 67.8, 114.6, 122.1, 126.5, 127.1, 128.5, 130.2, 131.4, 139.6, 145.8, 160.0; IR (ATR) cm^{-1} 3066.3, 2926.5, 2855.1, 1658.5, 1601.6, 1571.7, 1485.9, 1248.7, 1199.5, 1119.5, 1079.9, 1006.7, 970.0, 891.9, 835.0, 754.0, 725.1, 682.7, 603.6. HRMS (ESI/TOF-Q) m/z [6 + H]$^+$ calcd for $C_{31}H_{37}N_2O_3$, 485.2799; found, 485.2804.

1,3-Dihydro-4,5-bis[2′-(chloromethyl)phenyl]-2-(4″-octyloxyphenyl)imidazolium Chloride (7). To a solution of **6** (40 mg, 83 μmol) in CH_3CN (2 mL) was added $SOCl_2$ (30 μL, 0.42 mmol), and the mixture was stirred overnight at room temperature. After the solvent was removed, the remaining solid was dissolved in $CHCl_3$ to be poured in hexane to obtain **7** (55 mg, quantitative yield). Colorless solid; mp 112−113 °C; ^{1}H NMR (200 MHz, $CDCl_3$) δ ppm 0.79−1.06 (m, 3H), 1.34−1.58 (m, 10H), 1.86 (d, J = 6.57 Hz, 2H), 4.03 (t, J = 5.94 Hz, 2H), 4.68 (br s, 4H), 6.64−7.15 (m, 10H), 8.27 (d, J = 7.58 Hz, 2H), 14.33 (br s, 2H); ^{13}C NMR (50 MHz, $CDCl_3$) δ ppm 14.2, 22.7, 26.0, 29.4, 31.8, 44.8, 114.3, 115.0, 125.3, 128.0, 128.3, 130.5, 131.7, 137.2, 144.1, 162.4; IR (ATR) cm^{-1} 2925.5, 2855.1, 2696.0, 2617.9, 2586.1, 1643.1, 1611.2, 1504.2, 1474.3, 1297.9, 1019.2, 814.8, 764.6, 735.7, 677.9. HRMS (ESI/TOF-Q) m/z [7 − Cl]$^+$ calcd for $C_{31}H_{35}Cl_2N_2O$, 521.2126; found, 521.2121.

4-Octyloxyphenyl-Substituted Fused Imidazolium Chloride (2-Cl). To a solution of **7** (50 mg, 90 μmol) in DMF (10 mL) was added 1.0 M THF solution of LiHMDS (0.18 mL, 0.18 mmol) at 0 °C, and the mixture was stirred overnight at room temperature. After the solvent was removed, water and $CHCl_3$ were added in the separating funnel. An aqueous phase was extracted with $CHCl_3$. The combined organic phase was rinsed with saturated aqueous NH_4Cl and dried over $MgSO_4$. The solvent was removed and the remaining solid was dissolved in DMSO (10 mL) to be heated to 50 °C for 6 h. After the solvent was removed, the remaining solid was dissolved in $CHCl_3$ to be poured in ethyl acetate to obtain **2-Cl** (17 mg, 39% yield). Colorless solid; mp 254−256 °C; ^{1}H NMR (400 MHz, DMSO-d_6) δ ppm 0.83−0.94 (m, 3H), 1.23−1.37 (m, 8H), 1.42−1.48 (m, 2H), 1.68−1.85 (m, 2H), 4.16 (t, J = 6.40 Hz, 2H), 5.88 (s, 4H), 7.31 (d, J = 8.78 Hz, 2H), 7.51−7.68 (m, 4H), 7.76 (d, J = 7.53 Hz, 2H), 8.08−8.38 (m, 4H); ^{13}C NMR (100 MHz, DMSO-d_6) δ ppm 14.5, 22.6, 26.0, 29.0, 29.2, 31.7, 53.9, 68.7, 114.4, 116.0, 122.1, 124.7, 127.3, 129.1, 129.6, 129.7, 130.2, 138.4, 140.8, 162.2; IR (ATR) cm^{-1} 3389.3, 2926.5, 2847.4, 1599.7, 1463.7, 1270.9, 1187.9, 1003.8, 838.9, 756.9, 730.9, 715.5, 678.8, 645.1. HRMS (ESI/TOF-Q) m/z [**2-Cl** − Cl]$^+$ calcd for $C_{31}H_{33}N_2O$ 449.2587, found 449.2593. Anal. Calcd for $C_{31}H_{33}ClN_2O{\cdot}2H_2O$: C, 71.45; H, 7.16; N, 5.38. Found: C, 71.10; H, 6.93; N, 5.35.

4,5-Bis[2′-(hydroxymethyl)phenyl]-2-(4″- *N,N*-dibutylamino-phenyl)imidazole (8). From **5** (0.20 g, 0.40 mmol) and 4-(*N,N*-dibutylamino)benzaldehyde (0.17 g, 0.72 mmol), compound **8** was synthesized in a similar manner as **6** (0.10 g, 53% yield). Colorless solid; mp 75−76 °C; ^{1}H NMR (200 MHz, $CDCl_3$) δ ppm 0.89−0.97 (m, 6H), 1.32 (dd, J = 14.53, 7.20 Hz, 4H), 1.53 (d, J = 6.32 Hz, 4H), 3.18−3.33 (m, 4H), 4.54 (s, 4H), 6.62 (d, J = 8.34 Hz, 2H), 7.00−7.32 (m, 8H), 7.68 (d, J = 8.34 Hz, 2H), 9.59 (s,1H); ^{13}C NMR (50 MHz, $CDCl_3$) δ ppm 14.0, 22.3, 29.5, 50.8, 64.5, 110.8, 111.7, 116.2, 126.5, 127.9, 130.8, 133.0, 138.6, 146.1, 148.6, 152.8; IR (ATR) cm^{-1} 3063.4, 2954.4, 2929.3, 2859.9, 1613.2, 1501.3, 1455.1, 1402.0, 1365.4, 1286.3, 1198.5, 1110.8, 1002.8, 815.7, 761.7, 613.3. HRMS (ESI/TOF-Q) m/z [**8** + H]$^+$ calcd for $C_{31}H_{38}N_3O_2$, 484.2964; found, 484.2954.

1,3-Dihydro-4,5-bis[2′-(chloromethyl)phenyl]-2-(4″-*N,N*-dibutylaminophenyl)imidazolium Chloride (9). From **8** (80 mg, 0.17 mmol), compound **9** was synthesized in a similar manner as **7** (75 mg, 80% yield). Brown solid; mp 115−117 °C; ^{1}H NMR (200 MHz, $CDCl_3$) δ ppm 0.94 (br s, 6H), 1.31 (br s, 4H), 1.59 (br s, 4H), 3.37 (br s, 4H), 4.74 (br s, 4H), 7.07−7.54 (m, 10H), 8.53 (br s, 2H), 14.55 (br s, 1H); ^{13}C NMR (50 MHz, CD_3OD) δ ppm 12.7, 19.6, 27.9, 43.2, 62.0, 126.1, 128.7, 129.0, 130.7, 131.6, 137.6; IR (ATR) cm^{-1} 2959.2, 2925.5, 2870.5, 2702.7, 2572.6, 1642.1, 1606.4, 1509.1, 1259.3, 1143.6, 1052.9, 816.7, 765.6, 678.8, 606.5. HRMS (ESI/TOF-Q) m/z [**9** − Cl]$^+$ calcd for $C_{31}H_{36}Cl_2N_3$, 520.2286; found, 520.2284.

4-(*N,N*-Dibutylamino)phenyl-Substituted Fused Imidazolium Chloride (3-Cl). From **9** (40 mg, 70 μmol), compound **3-Cl** was synthesized in a similar manner as **2-Cl** (14 mg, 40% yield). Brown solid; mp 175−177 °C; ^{1}H NMR (400 MHz, DMSO-d_6) δ ppm 0.96 (t, J = 7.28 Hz, 6H), 1.33−1.41 (m, 4H), 1.54−1.61 (m, 4H), 3.45 (t, J = 7.40 Hz, 4H), 5.86 (s, 4H), 6.92 (d, J = 9.03 Hz, 2H), 7.59−7.68 (m, 4H), 7.75 (d, J = 7.53 Hz, 2H), 8.00 (d, J = 9.03 Hz, 2H), 8.23 (d, J = 7.53 Hz, 2H); ^{13}C NMR (100 MHz, CD_3OD) δ ppm 12.9, 19.8, 29.0, 50.3, 53.5, 106.8, 111.5, 121.2, 123.8, 127.2, 128.5, 128.9, 129.0, 139.3, 140.0, 150.8; IR (ATR) cm^{-1} 3366.1, 2961.2, 2932.2, 2871.5, 2716.3, 2587.0, 1640.2, 1605.5, 1509.1, 1374.0, 1259.3, 1212.1, 1157.1, 950.7, 816.7, 679.8, 620.1, 608.4. HRMS (ESI/TOF-Q) m/z [**3-Cl** − Cl]$^+$ calcd for $C_{31}H_{34}N_3$, 448.2753; found, 448.2780. Anal. Calcd for $C_{31}H_{34}ClN_3{\cdot}4H_2O$: C, 66.95; H, 7.61; N, 7.56. Found: C, 66.69; H, 7.44; N, 7.64.

4,5-Bis[2′-(hydroxymethyl)phenyl]-2-(4″-trifluoromethyl-phenyl)imidazole (10). From **5** (0.30 g, 0.60 mmol) and 4-trifluoromethylbenzaldehyde (0.20 g, 1.2 mmol), compound **10** was synthesized in a similar manner as **6** (80 mg, 32% yield). Colorless solid; mp 205−206 °C; ^{1}H NMR (200 MHz, DMSO-d_6) δ ppm 4.26 (br s, 2H), 4.56 (br s, 2H), 5.25 (br s, 1H), 5.88 (br s, 1H), 6.84−7.18 (m, 2H), 7.27−7.65 (m, 6H), 7.92 (d, J = 8.08 Hz, 2H), 8.24 (d, J = 8.08 Hz, 2H), 13.23 (br s, 1H); ^{13}C NMR (50 MHz, DMSO-d_6) δ ppm 65.2, 125.8, 126.5, 128.6, 134.1, 143.7; IR (ATR) cm^{-1} 3168.5, 3073.0, 3053.7, 2940.0, 1621.8, 1589.1, 1461.8, 1436.7, 1323.9, 1251.6, 1174.4, 1108.9, 1065.5, 1012.5, 983.5, 849.5, 758.9. HRMS (ESI/TOF-Q) m/z [**10** + H]$^+$ calcd for $C_{24}H_{20}F_3N_2O_2$, 447.1477; found, 447.1496.

1,3-Dihydro-4,5-bis[2′-(chloromethyl)phenyl]-2-(4″-trifluoromethylphenyl)imidazolium Chloride (11). From **10** (70 mg, 0.22 mmol), compound **11** was synthesized in a similar manner as **7** (80 mg, 94% yield). Colorless solid; mp 260−261 °C; ^{1}H NMR (200 MHz, DMSO-d_6) δ ppm 4.88 (br s, 4H), 7.30−7.39 (m, 4H), 7.47 (t, J = 6.97 Hz, 2H), 7.62 (d, J = 7.58 Hz, 2H), 8.00 (d, J = 8.31 Hz, 2H), 8.38−8.45 (m, 2H); ^{13}C NMR (50 MHz, DMSO-d_6) δ ppm 44.7, 126.6, 127.4, 129.2, 131.2, 131.8, 137.3, 143.6; IR (ATR) cm^{-1} 3853.1, 3734.5, 3710.4, 3648.7, 3628.4, 3053.7, 2866.7, 2836.8, 2533.0, 1748.1, 1620.9, 1508.1, 1399.1, 1174.4, 1017.3, 816.8, 681.7. HRMS (ESI/TOF-Q) m/z [**11** − Cl]$^+$ calcd for $C_{24}H_{18}Cl_2F_3N_2$, 461.0799; found, 461.0794.

4-Trifluoromethylphenyl-Substituted Fused Imidazolium Chloride (4-Cl). From **11** (80 mg, 0.16 mmol), compound **4-Cl** was synthesized in a similar manner as **2-Cl** (14 mg, 40% yield). Colorless solid; mp 313−315 °C; ^{1}H NMR (400 MHz, DMSO-d_6) δ ppm 5.97 (s, 4H), 7.59−7.74 (m, 4H), 7.79 (d, J = 7.28 Hz, 2H), 8.18 (d, J = 8.28 Hz, 2H), 8.31 (d, J = 7.53 Hz, 2H), 8.49 (d, J = 8.28 Hz, 2H); ^{13}C NMR (100 MHz, DMSO-d_6) δ ppm 54.1, 122.4, 124.8, 127.2, 129.4, 129.7, 130.1, 130.2, 137.0, 140.8; IR (ATR) cm^{-1} 3524.7, 3396.3, 3360.4, 3017.1, 2926.5, 1711.5, 1619.9, 1476.3, 1170.7, 1009.6, 946.9, 892.9, 857.2, 780.1, 731.9, 722.2, 658.6. HRMS (ESI/TOF-Q) m/z [**4-Cl** − Cl]$^+$ calcd for $C_{24}H_{16}F_3N_2$, 389.1260; found, 389.1268. Anal. Calcd for $C_{24}H_{16}ClF_3N_2{\cdot}2.5H_2O$: C, 61.35; H, 4.50; N, 5.96. Found: C, 61.10; H, 4.33; N, 5.80.

4,5-Bis[2′-(hydroxymethyl)phenyl]-2-(4″-cyanophenyl)-imidazole (12). From **5** (0.15 g, 0.30 mmol) and 4-cyanobenzaldehyde (50 mg, 0.39 mmol), compound **12** was synthesized in a similar manner as **6** (70 mg, 31% yield). Brown solid; mp 125−127 °C; ^{1}H NMR (400 MHz, $CDCl_3$) δ ppm 4.69 (br s, 4H), 7.15 (br s, 4H), 7.27−7.33 (m, 2H), 7.45 (d, J = 7.53 Hz, 2H), 7.69 (d, J = 8.53 Hz, 2H), 7.90 (s, 2H); ^{13}C NMR (50 MHz, $CDCl_3$) δ ppm 64.7, 111.3, 111.7, 125.3, 127.4, 128.1, 128.3, 131.8, 132.9, 133.3, 142.8, 143.5; IR (ATR) cm^{-1} 3194.5, 2938.9, 2847.4, 2226.4, 1609.3, 1486.9, 1440.5, 1220.5, 1001.8, 972.9, 842.7, 763.7, 695.2, 607.5. HRMS (ESI/TOF-Q) m/z [**12** + Na]$^+$ calcd for $C_{24}H_{19}N_3NaO_2$, 404.1375; found, 404.1380.

1,3-Dihydro-4,5-bis[2′-(chloromethyl)phenyl]-2-(4″-cyanophenyl)imidazolium Chloride (13). From **12** (80 mg, 0.22

DOI: 10.1021/acs.joc.5b01028
J. Org. Chem. 2015, 80, 7172−7183

mmol), compound **13** was synthesized in a similar manner as **7** (65 mg, 64% yield). Brown solid; mp 189−191 °C; ^{1}H NMR (200 MHz, CD_3OD) δ ppm 4.65 (s, 4H), 7.52−7.68 (m, 8H), 8.08−8.17 (m, 2H), 8.23−8.30 (m, 2H); ^{13}C NMR (50 MHz, CD_3OD) δ ppm 43.2, 115.6, 117.2, 125.7, 127.7, 129.0, 130.8, 131.6, 133.3, 137.7, 143.1; IR (ATR) cm^{-1} 2866.7, 2843.5, 2719.1, 2374.9, 2342.1, 1717.3, 1642.1, 1610.3, 1399.1, 1264.1, 902.5, 842.7, 767.5, 603.6. HRMS (ESI/TOF-Q) m/z [**13** − Cl]$^+$ calcd for $C_{24}H_{18}Cl_2N_3$, 418.0872; found, 418.0869.

4-Cyanophenyl-Substituted Fused Imidazolium Chloride (5-Cl). From **13** (55 mg, 0.12 mmol), compound **5-Cl** was synthesized in a similar manner as **2-Cl** (10 mg, 22% yield). Brown solid; mp 335−337 °C; ^{1}H NMR (400 MHz, DMSO-d_6) δ ppm 5.97 (s, 4H), 7.63−7.73 (m, 4H), 7.79 (d, J = 7.28 Hz, 2H), 8.29−8.35 (m, 4H), 8.45 (d, J = 8.53 Hz, 2H); ^{13}C NMR was not available due to low solubility; IR (ATR) cm^{-1} 3092.3, 3053.7, 2696.0, 2533.1, 2475.2, 1634.4, 1499.4, 1387.5, 1127.2, 1043.3, 898.7, 764.6, 753.1, 670.1, 610.4. HRMS (ESI/TOF-Q) m/z [**5-Cl** − Cl]$^+$ calcd for $C_{24}H_{16}N_3$, 346.1339; found, 346.1339. Anal. Calcd for $C_{24}H_{16}ClN_3\cdot 1.6H_2O$: C, 70.19; H, 4.71; N, 10.23. Found: C, 70.03; H, 4.64; N, 10.19.

4-Octyloxyphenyl-Substituted Fused Imidazolium Bis(trifluoromethanesulfonyl)imidate (2-TFSI). To a solution of **1-Cl** (10 mg, 21 μmol) in $CHCl_3$ (1.2 mL) was added a solution of LiTFSI (0.46 g, 1.6 mmol) in distilled water (1.6 mL), and the mixture was stirred overnight at room temperature. An aqueous phase was extracted with $CHCl_3$. The combined organic phase was dried over $MgSO_4$ to be poured in hexane to obtain **2-TFSI** (15 mg, quantitative yield). Colorless solid; mp 126−127 °C; ^{1}H NMR (400 MHz, $CDCl_3$) δ ppm 0.82−0.99 (m, 3H), 1.25−1.46 (m, 10H), 1.77 (d, J = 6.57 Hz, 2H), 3.98 (t, J = 6.44 Hz, 2H), 5.51 (s, 4H), 7.14 (d, J = 8.84 Hz, 2H), 7.40−7.67 (m, 6H), 7.77 (d, J = 7.33 Hz, 2H), 7.88 (d, J = 8.59 Hz, 2H); ^{13}C NMR (100 MHz, CD_3OD) δ ppm 13.0, 22.3, 25.7, 28.8, 29.0, 29.1, 31.6, 53.2, 68.3, 115.6, 121.5, 123.8, 127.3, 129.1, 140.0; IR (ATR) cm^{-1} 2939.9, 2857.1, 1603.5, 1475.3, 1336.4, 1313.3, 1267.1, 1182.2, 1128.2, 760.8, 727.1, 661.5. HRMS (ESI/TOF-Q) m/z [TFSI]$^-$ calcd for $C_2F_6NO_4S_2$, 279.9173; found, 279.9178. Anal. Calcd for $C_{33}H_{33}F_6N_3O_5S_2$: C, 54.31; H, 4.56; N, 5.76; S, 8.79; Found: C, 54.14; H, 4.60; N, 5.43; S, 8.95.

4-Octyloxyphenyl-Substituted Fused Imidazolium Tetrafluoroborate (2-BF4). To a solution of **1-Cl** (30 mg, 62 μmol) in AN (1.9 mL) was added a 1 M CH_2Cl_2 solution of Et_3OBF_4 (62 μL, 62 μmol), and the mixture was stirred overnight at room temperature. After the solid was filtered, the filtrate was evaporated to give yellow solid that was recrystallized from $CHCl_3$/hexane to obtain **2-BF4** (20 mg, 60% yield). Pale yellow solid; mp 235−236 °C; ^{1}H NMR (400 MHz, $CDCl_3$) δ ppm 0.89−0.93 (m, 3H), 1.33 (br s, 10H), 1.67−1.84 (m, 2H), 3.75 (t, J = 6.53 Hz, 2H), 5.42 (s, 4H), 6.98 (d, J = 8.53 Hz, 2H), 7.30−7.45 (m, 4H), 7.62 (dd, J = 16.82, 6.53 Hz, 4H) 7.90 (d, J = 8.53 Hz, 2H); ^{13}C NMR (100 MHz, $CDCl_3$) δ ppm 14.1, 22.7, 25.9, 29.0, 29.3, 29.4, 31.6, 31.8, 54.1, 68.6, 112.9, 116.0, 121.2, 124.8, 126.7, 129.2, 129.4, 129.7, 139.5, 162.5; IR (ATR) cm^{-1} 2923.6, 2840.7, 1606.4, 1488.8, 1463.7, 1445.4, 1310.4, 1291.1, 1263.2, 1180.2, 1029.8, 896.7, 843.7, 809.9, 776.3, 727.1, 679.8. HRMS (ESI/TOF-Q) m/z [BF_4]$^-$ calcd for BF_4, 87.0029; found, 87.0029; Anal. Calcd for $C_{31}H_{33}BF_4N_2O\cdot H_2O$: C, 67.16; H, 6.36; N, 5.05; Found: C, 67.42; H, 6.19; N, 5.11.

4,7-Dibromo-2-(4′-*N*,*N*-dibutylaminophenyl)-1*H*-benzimidazole (14). To a solution of 3,6-dibromo-1,2-phenylenediamine (1.7 g, 6.4 mmol) and *N*,*N*-dibutylbenzaldehyde (2.0 g, 8.3 mmol) in $CHCl_3$ (70 mL) was added $ZrCl_4$ (0.14 g, 0.64 mmol), and the mixture was stirred for 4 days at room temperature. After the solid was filtered, the filtrate was evaporated to give a yellow solid that was recrystallized from $CHCl_3$/AN to obtain **14** (1.5 g, 43% yield). Colorless solid; mp 239−240 °C; ^{1}H NMR (200 MHz, DMSO-d_6) δ ppm 0.83−0.98 (m, 6H), 1.32−1.68 (m, 8H), 6.76 (d, J = 8.84 Hz, 2H), 7.28 (s, 2H), 8.10 (d, J = 8.59 Hz, 2H); ^{13}C NMR (100 MHz, DMSO-d_6) δ ppm 14.3, 20.1, 29.5, 50.3, 111.4, 115.1, 125.9, 129.5, 150.0, 154.6; IR (ATR) cm^{-1} 3901.3, 3735.4, 3073.1, 2955.4, 2869.6, 2777.9, 1607.4, 1494.6, 1470.5, 1305.6, 1169.6, 1110.8, 927.6, 757.9, 700.1. HRMS (ESI/TOF-Q) m/z [**14** + H]$^+$ calcd for $C_{21}H_{26}Br_2N_3$, 478.0493; found, 478.0493.

2-(4″-*N*,*N*-Dibutylaminophenyl)-4,7-bis(2′-hydroxymethylphenyl)benzimidazole (15). To a solution of **14** (1.3 g, 2.7 mmol) and 2-hydroxymethylphenylboronic acid (0.9 g, 5.9 mmol) in THF (100 mL) were added 2 M aqueous Na_2CO_3 (9.0 mL) and $Pd(PPh_3)_4$ (0.47 g, 0.41 mmol), and the mixture was heated to reflux overnight. After the solvent was removed, water and ethyl acetate were added in the separating funnel. An aqueous phase was extracted with ethyl acetate. The combined organic phase was rinsed with saturated aqueous NH_4Cl and dried over $MgSO_4$. The solvent was removed and the remaining solid was recrystallized from $CHCl_3$/AN to obtain **15** (0.38 g, 26% yield). Colorless solid; mp 169−170 °C; ^{1}H NMR (200 MHz, $CDCl_3$) δ ppm 0.82−0.91 (m, 6H), 1.22−1.50 (m, 8H), 3.19 (t, J = 7.20 Hz, 4H), 4.51 (br s, 4H), 6.47 (d, J = 8.34 Hz, 2H), 7.26 (s, 2H), 7.46 (br s, 6H), 7.55−7.67 (m, 4H); ^{13}C NMR (100 MHz, DMSO-d_6) δ ppm 14.3, 20.1, 29.4, 50.2, 79.7, 111.3, 116.2, 123.4, 127.3, 128.0, 129.0, 130.9, 141.0, 149.5, 153.7; IR (ATR) cm^{-1} 3853.1, 3734.5, 3063.4, 2955.4, 2859.9, 1609.3, 1490.7, 1398.1, 1363.4, 1285.3, 1200.5, 1001.8, 926.6, 819.6, 756.9. HRMS (ESI/TOF-Q) m/z [**15** + H]$^+$ calcd for $C_{35}H_{40}N_3O_2$, 534.3121; found, 534.3121.

1,3-Dihydro-4,7-bis(2′-chloromethylphenyl)-2-(4″-*N*,*N*-dibutylaminophenyl)benzimidazolium Chloride (16). To a solution of **15** (0.33 g, 0.62 mmol) in CH_3CN (50 mL) was added $SOCl_2$ (0.22 mL, 3.1 mmol), and the mixture was stirred overnight at room temperature. After the solvent was removed, the remaining solid was dissolved in $CHCl_3$ to be poured in hexane to obtain **16** (0.28 g, 74% yield). Brown solid; mp 135−136 °C; ^{1}H NMR (200 MHz, $CDCl_3$) δ ppm 0.93−1.00 (m, 6H), 1.33 (br s, 8H), 3.34 (br s, 4H), 4.63 (br s, 4H), 6.86 (br s, 2H), 7.42−7.76 (m, 10H), 8.44 (br s, 2H); ^{13}C NMR (100 MHz, DMSO-d_6) δ ppm 14.3, 20.0, 29.3, 45.0, 50.4, 111.4, 125.6, 126.7, 129.4, 129.6, 131.1, 131.3, 131.6, 136.3, 136.7, 152.4; IR (ATR) cm^{-1} 3854.1, 3750.9, 3676.6, 3648.7, 3023.8, 2956.3, 2925.5, 2859.9, 2637.2, 2568.7, 2500.3, 1604.5, 1509.1, 1457.9, 1289.2, 1208.2, 926.6, 819.6, 669.2. HRMS (ESI/TOF-Q) m/z [**16** − Cl]$^+$ calcd for $C_{35}H_{38}Cl_2N_3$, 570.2437; found, 570.2443.

4-(*N*,*N*-Dibutylamino)phenyl-Substituted Fused Benzimidazolium Chloride (6-Cl). To a solution of **16** (0.10 g, 0.17 mmol) in DMF (22 mL) was added 1.0 M THF solution of LiHMDS (0.38 mL, 0.38 mmol) at 0 °C, and the mixture was stirred overnight at room temperature. After the solvent was removed, water and $CHCl_3$ were added in the separating funnel. An aqueous phase was extracted with $CHCl_3$. The combined organic phase was rinsed with saturated aqueous NH_4Cl and dried over $MgSO_4$. The solvent was removed and the remaining solid was dissolved in DMSO (12 mL) to be heated to 50 °C for 6 h. After the solvent was removed, the remaining solid was washed with ethyl acetate to obtain **6-Cl** (50 mg, 59% yield). Brown solid; mp 229−231 °C; ^{1}H NMR (400 MHz, CD_3OD) δ ppm 1.06 (t, J = 7.40 Hz, 6H), 1.44−1.56 (m, 4H), 1.72 (quintet, J = 7.59 Hz, 4H), 3.49−3.58 (m, 4H), 5.86 (s, 4H), 7.05 (d, J = 9.03 Hz, 2H), 7.38−7.52 (m, 6H), 7.83−7.91 (m, 4H), 8.04 (d, J = 6.78 Hz, 2H); ^{13}C NMR (100 MHz, DMSO-d_6) δ ppm 14.4, 20.1, 29.4, 48.1, 50.4, 79.8, 105.4, 111.8, 118.9, 119.9, 123.8, 126.4, 126.9, 128.6, 129.0, 130.0, 131.5, 148.5, 151.3; IR (ATR) cm^{-1} 3854.1, 3819.3, 3750.9, 3711.3, 3676.6, 3648.7, 2948.6, 2929.3, 2861.8, 1716.3, 1558.2, 1465.6, 1204.3, 879.4, 825.4, 744.4, 695.2. HRMS (ESI/TOF-Q) m/z [**6-Cl** − Cl]$^+$ calcd for $C_{35}H_{36}N_3$, 498.2904; found, 498.2927. Anal. Calcd for $C_{35}H_{36}ClN_3\cdot 4H_2O$: C, 69.35; H, 7.32; N, 6.93; Found: C, 69.47; H, 7.26; N, 6.83.

4,7-Dibromo-2-(4′-cyanophenyl)-1*H*-benzimidazole (17). From 3,6-dibromo-1,2-phenylenediamine[3] (1.5 g, 5.6 mmol) and 4-cyanobenzaldehyde (0.87 g, 6.7 mmol), compound **17** was synthesized in a similar manner as **14** (1.7 g, 81% yield). Colorless solid; ^{1}H NMR (200 MHz, DMSO-d_6) δ ppm 7.47 (s, 2H), 8.09 (d, J = 8.34 Hz, 2H), 8.55 (d, J = 8.34 Hz, 2H); ^{13}C NMR (100 MHz, DMSO-d_6) δ ppm 79.7, 113.0, 118.9, 127.1, 128.5, 133.1, 133.6, 151.5; IR (ATR) cm^{-1} 3902.3, 3854.1, 3819.3, 3750.9, 3711.3, 3675.7, 3215.7, 2240.9, 1698.1, 1558.2, 1540.9, 1488.8, 1473.4, 1298.8, 1176.4, 842.7, 756.9, 668.2. HRMS (ESI/TOF-Q) m/z [**17** + H]$^+$ calcd for $C_{14}H_8Br_2N_3$, 377.9085; found, 377.9068.

2-(4″-Cyanophenyl)-4,7-bis(2′-hydroxymethylphenyl)-1*H*-benzimidazole (18). From **17** (1.0 g, 2.7 mmol), compound **18** was synthesized in a similar manner as **15** (0.50 g, 43% yield). Colorless

DOI: 10.1021/acs.joc.5b01028
J. Org. Chem. 2015, 80, 7172−7183

solid; mp 171−172 °C; ^{1}H NMR (200 MHz, DMSO-d_6) δ ppm 4.38−4.52 (m, 4H), 5.09−5.30 (m, 2H), 7.20 (s, 2H), 7.34−7.51 (m, 6H), 7.61−7.78 (m, 2H), 7.95 (d, J = 8.08 Hz, 2H), 8.34 (d, J = 8.08 Hz, 2H), 12.82 (s, 1H); ^{13}C NMR (100 MHz, DMSO-d_6) δ ppm 61.5, 112.4, 119.1, 127.1, 127.9, 128.2, 130.6, 133.1, 134.5, 141.1, 150.7; IR (ATR) cm^{-1} 3854.1, 3820.3, 3675.7, 3629.4, 3282.3, 3133.8, 3033.5, 2228.3, 1698.1, 1683.6, 1652.7, 1609.3, 1520.6, 1456.9, 1198.4, 984.5, 834.1, 756.9, 681.7. HRMS (ESI/TOF-Q) m/z [**18** + Na]$^+$ calcd for $C_{28}H_{21}N_3NaO_2$, 454.1531; found, 454.1537.

1,3-Dihydro-4,7-bis(2′-chloromethylphenyl)-2-(4″-cyanophenyl)-1*H*-benzimidazolium Chloride (19). The compound was synthesized From **18** (0.40 g, 0.93 mmol), compound **19** was synthesized in a similar manner as **16** (0.40 g, 85% yield). Colorless solid; mp 278−279 °C; ^{1}H NMR (400 MHz, DMSO-d_6) δ ppm 4.74 (s, 4H), 7.34 (s, 2H), 7.49−7.58 (m, 6H), 7.67−7.75 (m, 2H), 7.97 (d, J = 8.34 Hz, 2H), 8.34 (d, J = 8.34 Hz, 2H); ^{13}C NMR (100 MHz, DMSO-d_6) δ ppm 45.2, 113.5, 118.9, 125.6, 129.1, 129.3, 131.0, 131.4, 133.0, 136.5, 137.5, 150.9; IR (ATR) cm^{-1} 3092.3, 3053.7, 2696.0, 2533.1, 2475.2, 2232.2, 1634.4, 1499.4, 1387.5, 1127.2, 1043.3, 898.7, 764.6, 753.1, 670.1, 610.4. HRMS (ESI/TOF-Q) m/z [**19** − Cl]$^+$ calcd for $C_{28}H_{20}Cl_2N_3$, 468.1029; found, 468.1042.

4-Cyanophenyl-Substituted Fused Benzimidazolium Chloride (7-Cl). From **19** (0.20 g, 0.40 mmol), compound **7-Cl** was synthesized in a similar manner as **6-Cl** (65 mg, 38% yield). Yellow solid; mp 227−228 °C; ^{1}H NMR (400 MHz, CD_3OD) δ ppm 5.94 (s, 4H), 7.42−7.56 (m, 6H), 8.18 (s, 2H), 8.24−8.29 (m, 2H), 8.37 (s, 4H); ^{13}C NMR was not available due to low solubility; IR (ATR) cm^{-1} 3853.1, 3734.5, 3648.7, 3335.3, 2981.4, 2941.9, 2224.9, 165.7, 1540.9, 1472.4, 1364.4, 1008.6, 842.7, 762.7, 685.6. HRMS (ESI/TOF-Q) m/z [**7-Cl** − Cl]$^+$ calcd for $C_{28}H_{18}N_3$, 396.1495; found, 396.1512. Anal. Calcd for $C_{28}H_{18}ClN_3\cdot1.5H_2O$: C, 73.28; H, 4.61; N, 9.16; Found: C, 73.38; H, 4.46; N, 9.02.

COMPUTATIONAL DETAILS

Density Functional Theory Calculations. DFT calculations were performed with the Gaussian 09W (revision C.01) package of programs. The ground-state structure was optimized with DFT calculation at the B3LYP/6-31G(d) level of theory. The TD-DFT calculation was then performed at the B3LYP/6-311+G(d,p) level of theory to estimate the vertical excitation energy.

Symmetry-Adapted Cluster−Configuration Interaction Calculations. The SAC−CI[19] and PCM SAC−CI[20] calculations were performed by using D95(d) basis set. For absorption spectra, the ground-state geometries were optimized by the B3LYP/6-31G(d,p) method. For fluorescence spectra, the excited-state geometries were optimized by the TD PBE0/6-31G(d,p) method. The perturbation-selection thresholds were set to 1.0×10^{-7} and 1.0×10^{-8} for ground and excited states, respectively.[22] The direct SAC/SAC−CI[23] and SAC−CI NV methods were used for the SAC and SAC−CI equations. Integral equation formula (IEF) PCM[24] with the default parameters was used for considering the solvent effects. The corrected linear response PCM SAC−CI[25] was used for calculations of the absorption spectra, and the state-specific PCM SAC−CI[20] was used for calculations of the fluorescence spectra. The nonequilibrium solvation scheme was used for both absorption and emission.[26] The TD PBE0 and SAC−CI calculations were performed with the Gaussian 09 (revision C.01) package of programs,[27] and the PCM SAC−CI calculations were performed with the development version of Gaussian 09.

ASSOCIATED CONTENT

Supporting Information

Additional text describing materials and instrumentation; 19 figures showing ^{1}H NMR and ^{13}C NMR spectra; four figures and five tables showing DFT calculations, solvatochromism, influence of counteranion, and SAC−CI calculations; and listings of computational data. The Supporting Information is available free of charge on the ACS Publications website at DOI: 10.1021/acs.joc.5b01028.

AUTHOR INFORMATION

Corresponding Authors

*(K.T.) E-mail takagi.koji@nitech.ac.jp.
*(R.F.) E-mail fukuda@ims.ac.jp.

Notes

The authors declare no competing financial interest.

ACKNOWLEDGMENTS

This work was supported by Nanotechnology Platform Program (Molecule and Material Synthesis) of the Ministry of Education Culture, Sports, Science and Technology (MEXT), Japan. R.F. and M.E. acknowledge support from a Grant-in-Aid for Scientific Research from the Japan Society for the Promotion of Science (JSPS). Computations were performed in the Research Center for Computational Science, Okazaki, Japan.

REFERENCES

(1) (a) Scherf, U. *J. Mater. Chem.* **1999**, *9*, 1853−1864. (b) Watson, M. D.; Fechtenkötter, A.; Müllen, K. *Chem. Rev.* **2001**, *101*, 1267−1300. (c) Grimsdale, A. C.; Müllen, K. *Macromol. Rapid Commun.* **2007**, *28*, 1676−1702.

(2) (a) Jacob, J.; Sax, S.; Gaal, M.; List, E. J. W.; Grimsdale, A. C.; Müllen, K. *Macromolecules* **2005**, *38*, 9933−9938. (b) Thirion, D.; Poriel, C.; Rault-Berthelot, J.; Barrière, F.; Jeannin, O. *Chem.—Eur. J.* **2010**, *16*, 13646−13658.

(3) (a) Xiao, K.; Liu, Y.; Qi, T.; Zhang, W.; Wang, F.; Gao, J.; Qiu, W.; Ma, Y.; Cui, G.; Chen, S.; Zhan, X.; Yu, G.; Qin, J.; Hu, W.; Zhu, D. *J. Am. Chem. Soc.* **2005**, *127*, 13281−13286. (b) Usta, H.; Facchetti, A.; Marks, T. J. *Org. Lett.* **2008**, *10*, 1385−1388.

(4) (a) Sato, N.; Mazaki, Y.; Kobayashi, K.; Kobayashi, T. *J. Chem. Soc., Perkin Trans. 2* **1992**, 765−770. (b) Nenajdenko, V. G.; Sumerin, V. V.; Chernichenko, K. Y.; Balenkova, E. S. *Org. Lett.* **2004**, *6*, 3437−3439. (c) Zhang, X.; Côté, A. P.; Matzger, A. J. *J. Am. Chem. Soc.* **2005**, *127*, 10502−10503. (d) Okamoto, T.; Kudoh, K.; Wakamiya, A.; Yamaguchi, S. *Org. Lett.* **2005**, *7*, 5301−5304.

(5) (a) Bellina, F.; Cauteruccio, S.; Mannina, L.; Rossi, R.; Viel, S. *J. Org. Chem.* **2005**, *70*, 3997−4005. (b) Bellina, F.; Cauteruccio, S.; Fiore, A. D.; Rossi, R. *Eur. J. Org. Chem.* **2008**, 5436−5445. (c) Bellina, F.; Cauteruccio, S.; Fiore, A. D.; Marchetti, C.; Rossi, R. *Tetrahedron* **2008**, *64*, 6060−6072. (d) Monguchi, D.; Yamamura, A.; Fujiwara, T.; Somete, T.; Mori, A. *Tetrahedron Lett.* **2010**, *51*, 850−852.

(6) (a) Paul, A.; Mandal, P. K.; Samanta, A. *J. Phys. Chem. B* **2005**, *109*, 9148−9153. (b) Terashima, T.; Nakashima, T.; Kawai, T. *Org. Lett.* **2007**, *9*, 4195−4198. (c) Boydston, A. J.; Pecinovsky, C. S.; Chao, S. T.; Bielawski, C. W. *J. Am. Chem. Soc.* **2007**, *129*, 14550−14551. (d) Boydston, A. J.; Vu, P. D.; Dykhno, O. L.; Chang, V.; Wyatt, A. R., II; Stockett, A. S.; Ritschdorff, E. T.; Shear, J. B.; Bielawski, C. W. *J. Am. Chem. Soc.* **2008**, *130*, 3143−3156. (e) Nakashima, T.; Miyamura, K.; Sakai, T.; Kawai, T. *Chem. −Eur. J.* **2009**, *15*, 1977−1984. (f) Toba, M.; Nakashima, T.; Kawai, T. *Macromolecules* **2009**, *42*, 8068−8075. (g) Chen, X.-W.; Liu, J.-W.; Wang, J.-H. *J. Phys. Chem. B* **2011**, *115*, 1524−1530. (h) Binetti, E.; Panniello, A.; Triggiani, L.; Tommasi, R.; Agostiano, A.; Curri, M. L.; Striccoli, M. *J. Phys. Chem. B* **2012**, *116*, 3512−3518. (i) Hutt, J. T.; Jo, J.; Olasz, A.; Chen, C.-H.; Lee, D.; Aron, Z. D. *Org. Lett.* **2012**, *14*, 3162−3165. (j) Matsumoto, S.; Abe, H.; Akazome, M. *J. Org. Chem.* **2013**, *78*, 2397−2404.

(7) Nakashima, T.; Goto, M.; Kawai, S.; Kawai, T. *J. Am. Chem. Soc.* **2008**, *130*, 14570−14575.

(8) (a) Kouwer, P. H. J.; Swager, T. M. *J. Am. Chem. Soc.* **2007**, *129*, 14042−14052. (b) Shimura, H.; Yoshio, M.; Hoshino, K.; Mukai, T.; Ohno, H.; Kato, T. *J. Am. Chem. Soc.* **2008**, *130*, 1759−1765.

(9) (a) Powell, A. B.; Suzuki, Y.; Ueda, M.; Bielawski, C. W.; Cowley, A. H. *J. Am. Chem. Soc.* **2011**, *133*, 5218−5220. (b) Neilson, B. M.; Bielawski, C. W. *J. Am. Chem. Soc.* **2012**, *134*, 12693−12699.

(10) (a) Elie, C.-R.; Noujeim, N.; Pardin, C.; Schmitzer, A. R. *Chem. Commun.* **2011**, *47*, 1788−1790. (b) Elie, C.-R.; Hébert, A.;

DOI: 10.1021/acs.joc.5b01028
J. Org. Chem. 2015, 80, 7172−7183

Charbonneau, M.; Haiun, A.; Schmitzer, A. R. *Org. Biomol. Chem.* **2013**, *11*, 923−928.
(11) Takagi, K.; Ito, Y.; Kusafuka, K.; Sakaida, M. *Org. Biomol. Chem.* **2013**, *11*, 2245−2248.
(12) Methoxy (**2′-Cl**) and *N*,*N*-dimethylamino (**3′-Cl**) groups were used for decreasing the computation time. Only the fused π-conjugated imidazolium cation moieties were used for calculation (see ref 6f).
(13) For more accurate calculations, TD-DFT method using the range-separated functionals (i.e., LC-BLYP) might be required for these kinds of fused π-electron system. See Wong, B. M.; Hsieh, T. H. *J. Chem. Theory Comput.* **2010**, *6*, 3704−3712.
(14) (a) Mataga, N.; Kaifu, Y.; Koizumi, M. *Bull. Chem. Soc. Jpn.* **1956**, *29*, 465−470. (b) Lippert, E. *Z. Elektrochem.* **1957**, *61*, 962−975.
(15) Reichardt, C. *Chem. Rev.* **1994**, *94*, 2319−2358.
(16) Wiggins, K. M.; Kerr, R. L.; Chen, Z.; Bielawski, C. W. *J. Mater. Chem.* **2010**, *20*, 5709−5714.
(17) Nobuoka, K.; Kitaoka, S.; Kunimitsu, K.; Iio, M.; Harran, T.; Wakisaka, A.; Ishikawa, Y. *J. Org. Chem.* **2005**, *70*, 10106−10108.
(18) Hutt, J. T.; Jo, J.; Olasz, A.; Chen, C.-H.; Lee, D.; Aron, Z. D. *Org. Lett.* **2012**, *14*, 3162−3165.
(19) (a) Nakatusji, H.; Hirao, K. *J. Chem. Phys.* **1978**, *68*, 2053−2065. (b) Nakatsuji, H. *Chem. Phys. Lett.* **1978**, *59*, 362−364. (c) Nakatsuji, H. *Chem. Phys. Lett.* **1979**, *67*, 329−333. (d) Nakatsuji, H. *Chem. Phys. Lett.* **1979**, *67*, 334−342.
(20) Cammi, R.; Fukuda, R.; Ehara, M.; Nakatsuji, H. *J. Chem. Phys.* **2010**, *133*, No. 024104.
(21) Bahnous, M.; Mouats, C.; Fort, Y.; Gross, P. C. *Tetrahedron Lett.* **2006**, *47*, 1949−1951.
(22) Fukuda, R.; Ehara, M. *J. Comput. Chem.* **2014**, *35*, 2163−2176.
(23) Fukuda, R.; Nakatsuji, H. *J. Chem. Phys.* **2008**, *128*, No. 094105.
(24) (a) Cancès, E.; Mennucci, B.; Tomasi, J. *J. Chem. Phys.* **1997**, *107*, 3032−3041. (b) Mennucci, B.; Cancès, E.; Tomasi, J. *J. Phys. Chem. B* **1997**, *101*, 10506−10517. (c) Cancès, E.; Mennucci, B. *J. Math. Chem.* **1998**, *23*, 309−326.
(25) Fukuda, R.; Ehara, M.; Cammi, R. *J. Chem. Phys.* **2014**, *140*, No. 064114.
(26) Fukuda, R.; Ehara, M.; Nakatsuji, H.; Cammi, R. *J. Chem. Phys.* **2011**, *134*, No. 104109.
(27) Frisch, M. J.; et al.*Gaussian 09W*, revision C.01; Gaussian, Inc., Wallingford, CT, 2010 (see Supporting Information for full reference).

DOI: 10.1021/acs.joc.5b01028
J. Org. Chem. 2015, 80, 7172−7183